catalysts

MDPI

Article

Flow-Through Macroporous Polymer Monoliths Containing Artificial Catalytic Centers Mimicking Chymotrypsin Active Site

Mariia Stepanova [1], Olga Solomakha [1], Daria Ten [1], Tatiana Tennikova [2] and Evgenia Korzhikova-Vlakh [1,2,*]

[1] Institute of Macromolecular Compounds, Russian Academy of Sciences, 199004 St. Petersburg, Russia; maristepanova@hq.macro.ru (M.S.); solomanya@bk.ru (O.S.); dvendina@bk.ru (D.T.)
[2] Institute of Chemistry, Saint-Petersburg State University, 199034 St. Petersburg, Russia; tennikova@mail.ru
* Correspondence: vlakh@mail.ru; Tel.: +7-(812)-323-04-61

Received: 15 November 2020; Accepted: 28 November 2020; Published: 30 November 2020

Abstract: Synthetic catalysts that could compete with enzymes in term of the catalytic efficiency but surpass them in stability have a great potential for the practical application. In this work, we have developed a novel kind of organic catalysts based on flow-through macroporous polymer monoliths containing catalytic centers that mimic the catalytic site of natural enzyme chymotrypsin. It is known that chymotrypsin catalytic center consists of L-serine, L-histidine, and L-aspartic acid and has specificity to C-terminal residues of hydrophobic amino acids (L-phenylalanine, L-tyrosine, and L-tryptophan). In this paper, we have prepared the macroporous polymer monoliths bearing grafted polymer layer on their surface. The last one was synthesized via copolymerization of N-methacryloyl-L-serine, N-methacryloyl-L-histidine, and N-methacryloyl-L-aspartic acid. The spatial orientation of amino acids in the polymer layer, generated on the surface of monolithic framework, was achieved by coordinating amino acid-polymerizable derivatives with cobalt (II) ions without substrate-mimicking template and with its use. The conditions for the preparation of mimic materials were optimized to achieve a mechanically stable system. Catalytic properties of the developed systems were evaluated towards the hydrolysis of ester bond in a low molecular substrate and compared to the results of using chymotrypsin immobilized on the surface of a similar monolithic framework. The effect of flow rate increase and temperature elevation on the hydrolysis efficiency were evaluated for both mimic monolith and column with immobilized enzyme.

Keywords: macroporous polymer monoliths; enzyme mimics; artificial catalytic centers; molecular imprinting; flow-through catalysis; catalyzed hydrolysis

1. Introduction

Being biocatalysts, enzymes are widely used in many technological processes including food and drug industry, biotechnology, pulp and paper industry, etc. [1,2]. The catalytic efficiency of enzymes is very high. At the same time, the protein nature of enzymes is very sensitive to some conditions (organic solvents, pH, elevated temperature, etc.) and the catalytic activity can be easily lost due to distortion of the active site conformation. In addition, the time-consuming production and isolation of enzymes cause their high cost. In this regard, the development of artificial synthetic enzymes or moieties mimicking enzyme active site is the focus of many researches [3,4].

Currently, a number of enzyme mimics based on inorganics [5] or metal-organic frameworks (MOFs) [6,7] have been reported possessing with catalytic activity similar to that of enzymes. Mainly, inorganic systems and MOFs simulate the activity of oxidoreductases like peroxidase, superoxide

dismutase, glucose oxidase, and catalase [6,7]. Another group of enzymes that mimic with catalytic properties is based on the introduction of catalytically active groups into the polymeric matrix [8,9]. This technique is similar to molecular imprinting, the main idea of which is a formation of highly cross-linked polymer matrix around a template [3,10]. After the template removal, the created cavities match the template in terms of shape and functionality. Depending on the way of pre-polymerization complex formation, the covalent and noncovalent imprinting are distinguished. The variety of monomers makes it possible to design a polymer material with the ability to bind selectively the compound of interest with varying formats to be produced, e.g., polymer particles, films, or coatings. In the case of catalytic system preparation, a transition state analogue, a reaction intermediate, a substrate, or even a reaction product can be used as a template.

The preparation of artificial enzyme-mimic catalysts by molecular imprinting (molecularly imprinted catalysts, MICs) and their study have been reported in a number of original papers [11–14] and some reviews [4,15]. Among the mimicking enzymes, metalloproteinases [12,16] and hydrolases [14,17] can be mentioned. For instance, Tadi et al. developed a biosensor consisting of gold support covered with epinephrine-imprinted polymer microspheres obtained using hemin as catalytic centers to mimic active site of peroxidase and applied for the electrochemical detection of epinephrine [18]. A similar research was reported by Chen et al. who developed homovanillic acid-imprinted hemin-containing catalyst as peroxidase-mimic system in a form of nanogels [12]. An interesting approach to the preparation of peroxidase-mimic catalysts was recently published by Li et al. [13]. The authors used Fmoc-tripeptide and hemin for self-assembling monomers and template (2,2′-azinobis -(3-ethylbenzthiazoline-6-sulfonate)) to form the catalytic centers. As to hydrolase-mimicking catalysts, the design and study of chymotrypsin [14,19] and phosphotriesterase [17] MICs have been reported by some groups. In particular, Christy et al. fabricated chymotrypsin-mimics representing the catalytic imprinted polymer-bearing imidazole moiety on the surface of multiwalled carbon nanotubes [14]. Transition state analogue (TSA), phenyl 1-benzyloxycarbonylamino-4-methoxybenzyl phosphonate, was used as a template, and the catalytic activity of MICs was studied towards the hydrolysis of Z-L-phenylalanine p-nitrophenyl ester, which is specific low molecular substrate of chymotrypsin [17]. Lele at al. reported the preparation of microporous polymer beads, which contained chymotrypsin-mimicking catalytic centers. Those were prepared by grafting Co(II) coordinated monomer-template assemblies of various monomers possessing with hydroxyl, carboxyl, and imidazole functionalities. All MICs were found to be catalytically active towards chymotrypsin, specific substrate, namely, Z-L-tyrosine p-nitrophenyl ester [19]. Phosphotriesterase-mimics were recently prepared by Wang et al. who proposed the utilization of novel macrocyclic amine-type functional monomers to prepare MIC hollow nanoparticles for parathion (*O*,*O*-Diethyl *O*-(4-nitrophenyl)phosphorothioate) hydrolysis [17].

In most cases, the described artificial catalytic systems were designed as bead-based materials or coatings for inorganic surfaces. In this paper, we focused on the development of macroporous monolithic MICs. Macroporous polymer monoliths represent a continuous phase pierced with the interconnected flow-through channels or macropores [20,21]. This kind of materials is prepared via thermo- or photoinitiated polymerization of functional monomers in the presence of porogens in a mold. Nowadays, macroporous monoliths are widely used as stationary phases for many dynamic processes such as high-performance liquid chromatography [22,23], electrochromatography [24], gas chromatography [25], solid-phase extraction [26], and flow-through catalysis with immobilized enzymes [27]. Moreover, a number of works on the preparation and investigation of molecularly imprinted polymer monoliths for chromatography [28], solid-phase extraction [29], and microarray [30] can be found in the currently. The main advantage of macroporous monoliths over the bead-based stationary phases is their resistance to the high flow rates among with the very low backpressure. In turn, this provides the dominance of convective mechanism of mass transfer over the diffusion one inherent for columns packed with beads [31]. To the best of our knowledge, the preparation of macroporous monoliths with catalytic properties has not been previously reported.

In order to prepare macroporous monolithic MICs, we selected the chymotrypsin-mimic system and considered two strategies for generation catalytic centers. Co(II)-coordinated monomers containing hydroxyl, carboxyl, and imidazole groups and N-nicotinoyltyrosylbenzyl ester as a template were applied to create the chymotrypsin-mimicking active site. The catalytic properties of the developed mimics were evaluated with the use of Z-L-tyrosine p-nitrophenyl ester (Z-Tyr-OPNP) as known specific low molecular substrate for chymotrypsin. In addition, the catalytic properties of mimic monoliths were compared to those determined for chymotrypsin immobilized on the surface of monolithic column.

2. Results and Discussion

2.1. Preparation and Characterization of Macroporous Monolithic MICs

In contrast to the preparation of coatings and particles, the synthesis of macroporous monoliths is more complicated task. The polymerization mixture for the preparation of continuous media must satisfy to several requirements. First of all, besides monomers, template, and initiator, the polymerization mixture must contain porogenic solvents to generate a macroporous structure. To be porogenic, the solvents should be poor for the final polymer. At the same time, all components of the polymerization mixture must form a homogenous system. However, some components (monomers/templates/initiator) are solid compounds, which must be dissolved in the appropriate solvents. In turn, the introduction of a good solvent into the polymerization mixture can negatively affect the formation of a macroporous structure due to the increase in system compatibility. Finally, macroporous monoliths should be mechanically stable to resist the flow of the mobile phase.

It is well known that the catalytic site of chymotrypsin is formed by three key amino acids: Ser^{195}, Asp^{102}, and His^{57}. Therefore, the catalytic function of the enzyme is provided by three main functional groups: hydroxyl, carboxyl, and imidazole (Figure 1). The mechanism of enzymatically catalyzed hydrolysis of low-molecular-amino acid-based substrates is well known [32,33]. A schematic representation of the hydrolysis of N-modified tyrosine *p*-nitrophenyl ester catalyzed by chymotrypsin is shown in Figure 1.

In our case, the following monomers were selected to prepare macroporous monoliths containing these functional groups (Figure 2): (1) to provide imidazole functionality—N-methacryloyl-L-histidine (MA-His), (2) to provide carboxylic groups—methacrylic acid (MAA) or N-methacryloyl-L-aspartic acid (MA-Asp), and (3) to provide hydroxylic groups—2-hydroxyethyl methacrylate (HEMA) or N-methacryloyl-L-serine (MA-Ser). Ethylene glycol dimethacrylate (EDMA), poly(ethylene glycol) diacrylate (PEGDA), and di(ethylene glycol) dimethacrylate (DEGDMA) were tested as cross-linking monomers. It is known that to ensure the formation of macroporous structure and to obtain stable imprint sites, the polymerization mixture should contain at least 60 vol% of porogenic solvents and not less than 60 mol% of cross-linker from total amount of monomers [34].

Initially, attempts were made to synthesize nonimprinted macroporous monoliths using N-methacryloyl-L-histidine, methacrylic acid, 2-hydroxyethyl methacrylate, and EDMA/PEGDA, self-assembled into pre-polymerization complex with Co(II) ions. The tested compositions can be found in Table S1 of the Supplementary materials. Unfortunately, some of the tested polymerization mixtures were unstable and quickly delaminated, while others did not provide the necessary macroporous structure. The main problem when preparing a target catalytic system using a one-step approach was related to poor compatibility of components. The selected MAA and EDMA are moderately hydrophobic liquids, while $CoCl_2$ and MA-His are solid compounds, which are soluble in water and methanol, respectively. EDMA and MAA are poorly compatible with water so its amount should not be very high to avoid liquid–liquid separation. In turn, the introduction of hydrophobic solvents like toluene or 1-dodecanol as porogens favored to the rapid delamination of the system. Among the tested polymerization systems, only one consisting of MA-His/MAA/HEMA/EDMA = 10/10/10/70 (% mol/mol/mol/mol) (monomers), 10 mol% of $CoCl_2$ and 1,4-butanediol/methanol/water = 35/43/22

(% v/v/v) (porogens) allowed the formation of monoliths with necessary characteristics: the average pore size and porosity were equal to 1090 ± 85 nm and 90%, respectively. However, the mechanical properties of these monoliths were found to be inappropriate.

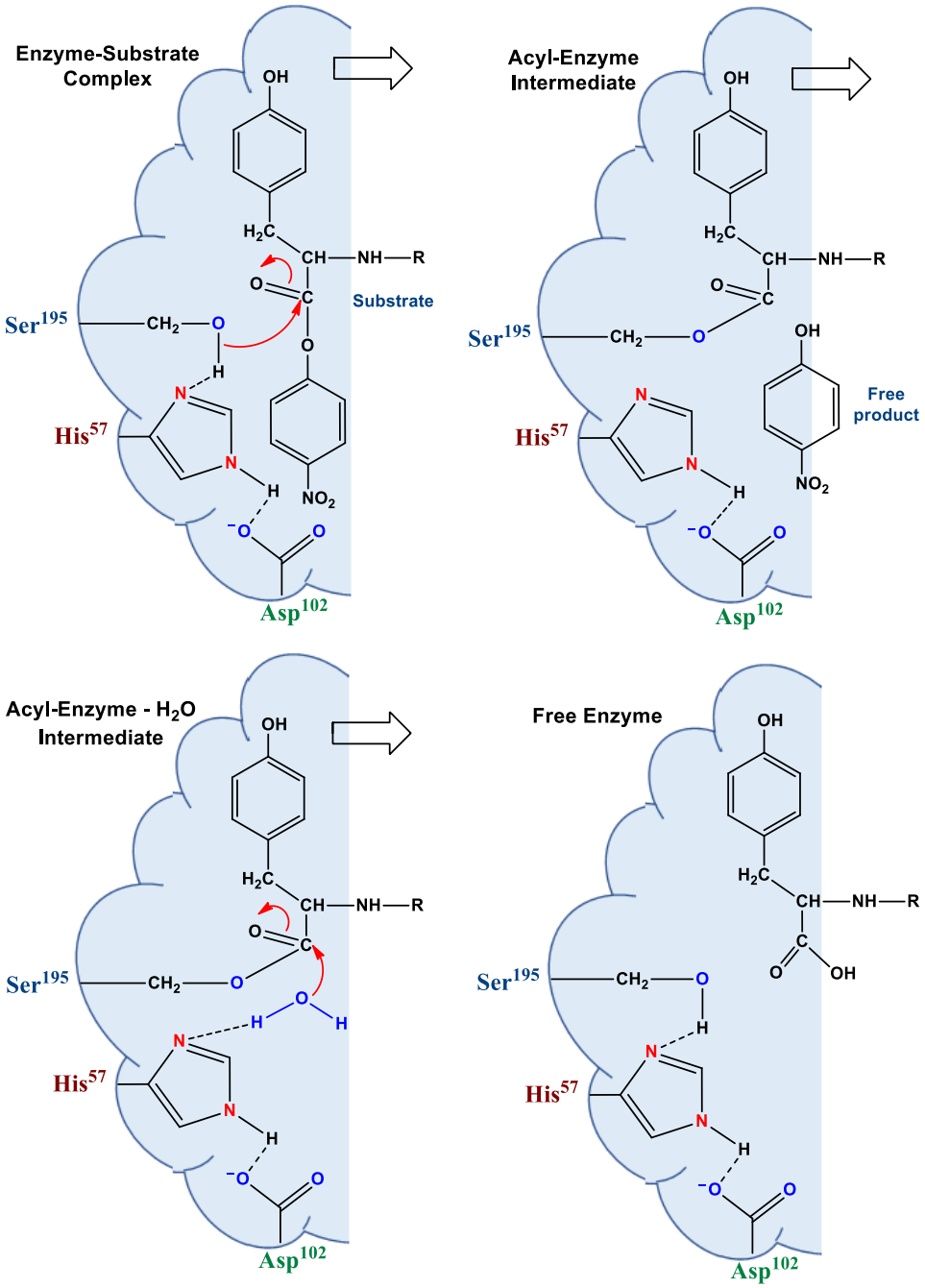

Figure 1. Scheme of N-modified tyrosine p-nitrophenyl ester hydrolysis catalyzed by chymotrypsin.

In order to overcome that problem, another approach to obtain macroporous monolithic mimics was proposed. The second way was based on a two-step approach, which included the preparation of macroporous monolithic framework with subsequent grafting of the functional layer on the surface of monolithic skeleton (Figure 3). In this case, the macroporous monolithic framework must be rigid and have a suitable pore size. All of the above advantages of monoliths can be realized with an average pore size of at least 1 μm. Since grafting the polymer layer on the walls of macropores can reduce the pore size, the initial pore size in monolithic framework should be not less than

1.5 µm. Given that framework performs only a supporting function, to simplify the preparation of monoliths, we used EDMA, DEGDMA, or PEGDA as a single monomer. Detailed information about the composition of the polymerization mixture and the characteristics of monoliths is given in Table S2 of the Supplementary materials. The monolith based on poly(ethylene glycol dimethacrylate) (poly(EDMA)) synthesized using 1-dodecanol/toluene = 70/30 (% v/v) as a porogenic mixture (sample 4, Table S2, the Supplementary Materials) was selected as the most suitable framework for further experiments on grafting.

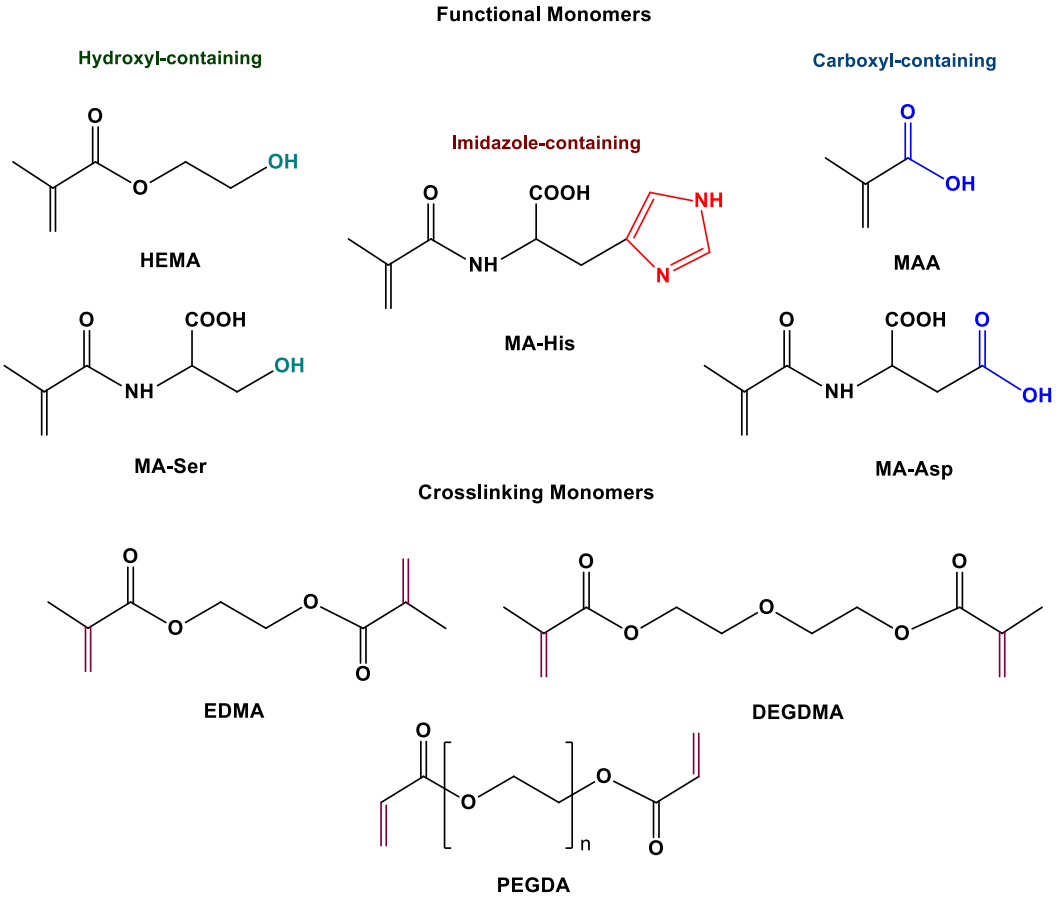

Figure 2. Structures of monomers and cross-linkers considered for preparation of macroporous mimic monoliths.

Grafting a polymer layer onto a macroporous polymer framework requires a certain amount of unreacted double bonds on the monolith surface. In this regard, it was necessary to choose the time of polymerization of the framework to achieve the required mechanical stability at dynamic flow of the mobile phase, on the one hand, and to preserve some double bonds for grafting, on the another one. In order to select the optimal time, the materials were prepared within 3, 4, 5, 6, and 9 h of polymerization. Residual surface double bonds were determined by Raman spectroscopy (Figure 4 and Figure S1 of the Supplementary Materials), where the characteristic band at 1639 cm^{-1} corresponded to the valent oscillation of the C=C group. As seen from the data presented in Figure 4, the amount of residual surface double bonds varied from 2.9% to 2.2% at the polymerization time of 3 and 9 h, respectively. Polymerization within 5 h was considered as optimal, since the shorter polymerization time did not provide the required rigidity (the monolith was compressed by 15–20% after a day of washing at flow rate of 1.0 $mL{\cdot}min^{-1}$). At the same time, after 5 h polymerization, about 2.5% of double bonds remained at monolith surface. The developed macroporous framework was characterized by an average pore size and total porosity of 1590 ± 80 nm and 82 ± 5%, respectively.

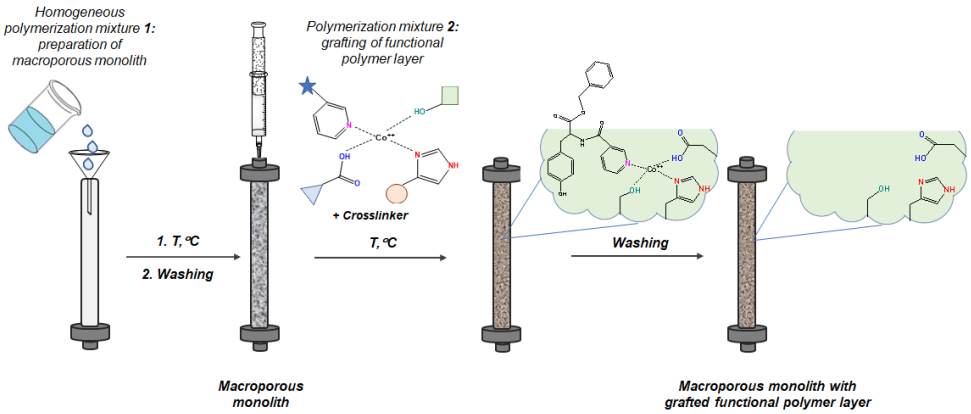

Figure 3. Scheme of the two-step preparation of macroporous monolithic molecularly imprinted catalysts mimicking chymotrypsin active site.

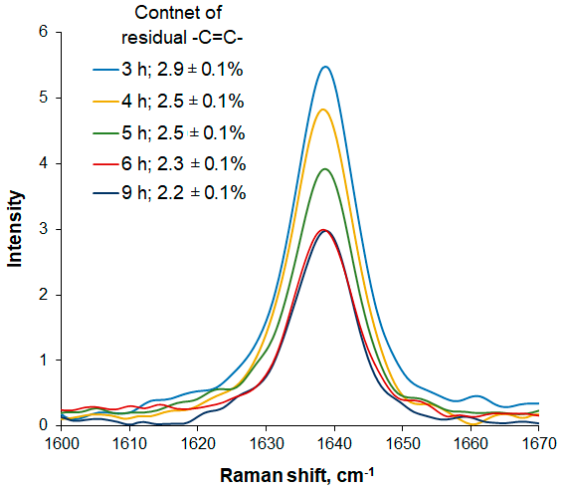

Figure 4. Fragment of Raman spectra illustrated bands corresponding to residual C=C groups for polyEDMA macroporous monoliths synthesized during different time.

Optimization of functional layer grafting was performed using MA-His, MAA, and HEMA as sources of imidazole, carboxyl, and hydroxyl functionalities and $CoCl_2$ as source of cobalt ions for coordination of the monomers. EDMA was used as a cross-linking monomer. At this step, we did not use the template. The formation of a Co(II)-coordinated assembly of stoichiometric amounts of monomers containing hydroxyl, carboxyl, and imidazole groups was previously testified by Lele at al. with the use of electron spin resonance (ESR) method [19]. As a result, formed assembly undergoes polymerization as a monomeric Co(II)-coordinated complex but not a random mixture of the three monomers.

The composition of the polymerization mixtures and the polymerization time used for grafting the functional layer are presented in Table 1. Methanol was used as a solvent for monomers and initiator. In all cases, we used equal amounts of functional monomers, whereas the amount of cross-linking monomer was different. Initially, we used equimolar quantities of components to prepare the grafted polymer layer. In this case, more or less appropriate grafting was achieved after 15 h of polymerization (sample 1). Two-three times better grafting of the functional layer was achieved with a threefold increase in the amount of cross-linking agent and a reduction in the polymerization time (sample 3). As expected, the grafting of the polymer layer on the surface of monoliths was accompanied by the slight decrease in their average pore size while the total porosity kept at the same level. In particular, the average pore size and porosity for samples 1, 2, and 3 were found to be 1480 ± 20, 1430 ± 50, and 1410 ± 20 nm and 81 ± 1, 75 ± 4 and 78 ± 4%, respectively.

Table 1. Compositions of polymerization mixtures used for grafting of polymer layer based on N-methacryloyl-L-histidine (MA-His), methacrylic acid (MAA), and ethylene glycol dimethacrylate (EDMA) and their time of polymerization and amounts of grafted MA-His.

Sample	Amount of Components, mmol					Grafting Time, h	Amount of Grafted MA-His **, μmol	
	$CoCl_2$	MA-His	MAA	HEMA	EDMA		Per 100 mg of Copolymer	Per Column
1	0.38	0.38	0.38	0.38	0.38	15	1.5 ± 0.1	4.6
2 *	0.38	0.38	0.38	0.38	1.14	5	–	–
3 *	0.38	0.38	0.38	0.38	1.14	8	2.1 ± 0.2	5.9

* the maximal quantities of components, which were managed to dissolve in 1.5 mL of methanol; ** determined by quantitative analysis of His released after acidic hydrolysis of amide bond between MA and His moieties (for details see Section 3.2.4).

The developed approach was applied to the synthesis of mimic layers on the surface of a macroporous monolithic material using MA-Asp and MA-Ser as functional monomers. Additionally, N-nicotinoyltyrosylbenzyl ester was introduced into polymerization mixture as a template. Functional monomers, template, and $CoCl_2$ were taken in equimolar quantities. Since the part of solid compounds, which must be dissolved for introduction into polymerization, was increased, the complete dissolution of the monomers and template in methanol was achieved at about 4 times reduced concentration. The polymerization was carried out for 8 h as previously optimized. The compositions of polymerization mixtures, as well as the characteristics of the prepared materials are given in Table 2. One can see that the introduction of Co(II) ions (nonimprinted catalyst (NIC)) as well as the template (molecularly imprinted catalyst (MIC)) favored to the higher inclusion of amino acid-based monomers in the grafted polymer layer. This result can be explained by the copolymerization of monomers in the Co(II)-assembled complex in the case of mimic systems (MIC and NIC) in contrast to the polymer formed from a disordered monomer mixture (control sample). Reducing the concentration of monomers provided the formation of a fairly thin grafted layer, which practically did not affect the average pore size. The average pore size was found to be 1560–1570 nm for all systems.

Table 2. Compositions of polymerization mixtures used for grafting of polymer layer based on MA-His, N-methacryloyl-L-aspartic acid (MA-Asp), and N-methacryloyl-L-serine (MA-Ser) as well as the amounts of grafted amino acid derivatives.

Column *	Amount of Components, mmol						Amount of Catalytic Centers **, μmol	
	$CoCl_2$	Template	MA-His	MA-Asp	MA-Ser	EDMA	Per 100 mg of Copolymer	Per Column
MIC	0.1	0.1	0.1	0.1	0.1	0.3	1.2 ± 0.3	2.6
NIC	0.1	–	0.1	0.1	0.1	0.3	0.7 ± 0.1	1.4
Control	–	–	0.1	0.1	0.1	0.3	0.3 ± 0.1	0.7

* polymerization time was 8 h; ** determined by quantitative analysis of amino acids released after acidic hydrolysis of amide bond between MA and amino acid moieties (for details see Section 3.2.4); the results of the analysis are given in terms of the number of catalytic sites where 3 equivalents of amino acids correspond to 1 equivalents of catalytic centers.

In addition, the morphology of the samples obtained was studied by the scanning electron microscopy (SEM). Figure 5 shows images of the surfaces of a macroporous framework and MIC monolithic material. The obtained images testify that all the monoliths were characterized by a homogeneous and fairly similar structure with a large number of interconnected macropores.

The mechanical stability of materials towards the flow of the mobile phase is one of the key properties of the flow-through systems. For monoliths, it is known that increasing the flow rate of the mobile phase increases the efficacy of dynamic interfacial processes, such as separation performance and the efficiency of biocatalytic processes based on immobilized enzymes [35,36]. The range of appropriate operating flow rates is determined by the linear interval of backpressure dependence on the flow rate of a mobile phase. Significant deviations from linearity, caused by backpressure growth,

may indicate mechanical instability leading to the destruction of macropores and compression of the material. In turn, an immediate reduction in backpressure may be a result of the monolith cracking.

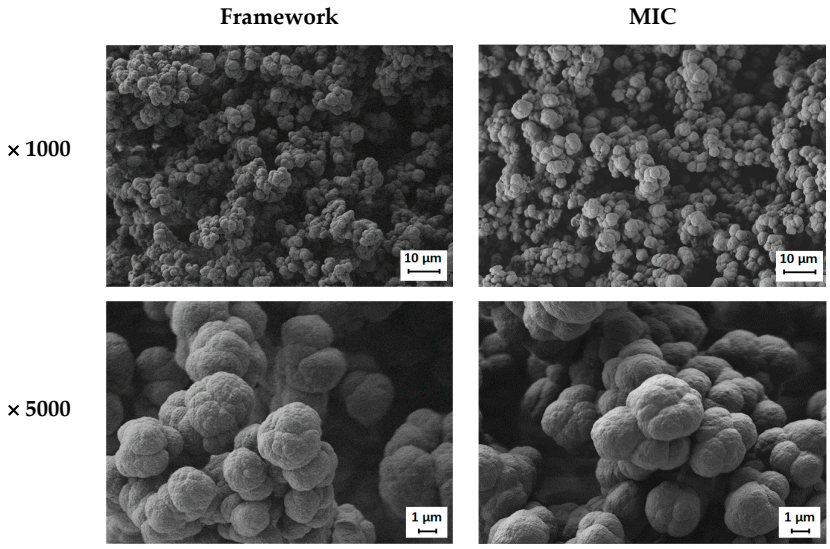

Figure 5. SEM images of macroporous monolithic framework and molecularly imprinted catalytic (MIC) monoliths.

Figure 6 illustrates the dependence of the backpressure on the flow rate for the developed MIC, NIC, control, and immobilized enzyme (IME) columns. A mixture of acetonitrile/water = 60/40 (% v/v) was used as the mobile phase. All tested materials showed a linear dependence of backpressure on flow rate up to 8.5 mL·min^{-1}. At this flow rate, the backpressure did not exceed 7.0 MPa. The result obtained clearly indicated that all materials were characterized by high mechanical stability towards the flow of mobile phase that agrees with tendency known for macroporous monoliths [35]. Moreover, this indirectly confirms that the grafted functional polymer is covalently fixed on the walls of the framework, but is not located inside the pores. Otherwise, the deviation from linearity would have occurred much earlier, and a significant increase in backpressure would have been observed due to the loss of material permeability caused by clogging the macropores by a polymer not attached to the framework.

A comparison of the tested columns discovers that the MIC column demonstrated an earlier deviation from linearity than other columns. This fact can be explained by the distortion of grafted layer whose quantity in MIC was higher than in NIC monolith.

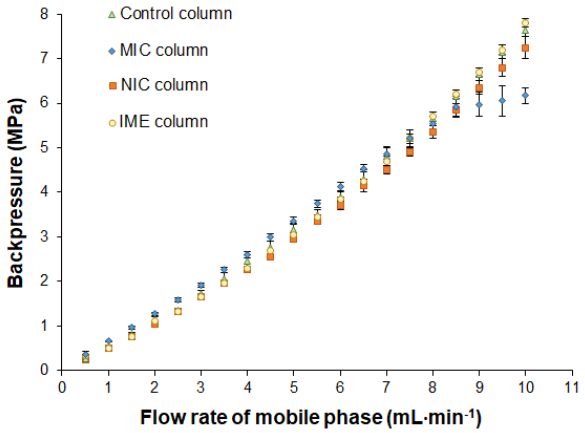

Figure 6. Dependence of backpressure on mobile phase flow rate for the different macroporous monolithic columns.

2.2. Study of Catalytical Properties

It is well known that chymotrypsin has specificity to ester and amide bonds formed with L-isomers of tyrosine, phenylalanine, and tryptophan [37]. In this study, hydrolytic activity of the prepared monoliths was studied towards chymotrypsin's low molecular substrate Z-Tyr-OPNP (Figure 7). In addition, Fmoc-Ala-OPNP (Figure 7) was used as a nonspecific substrate to evaluate the specificity of the developed chymotrypsin mimic systems towards aromatic amino acid-based substrates.

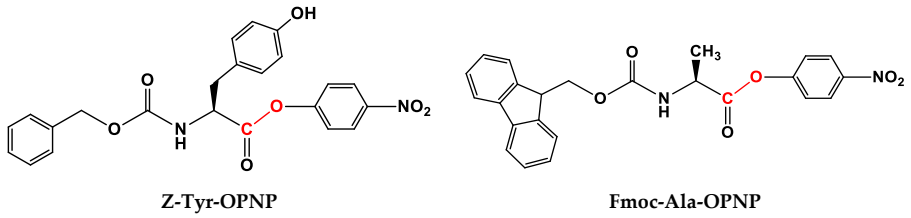

Figure 7. Structures of p-nitrophenyl esters of amino acid derivatives used as substrates.

Comparison of the substrate hydrolysis rate for MIC and NIC performed at 37 °C for 240 min to noncatalyzed system at the same conditions testified that both mimic monoliths surpassed the noncatalyzed hydrolysis (Figure 8A). Previously it was established that for monoliths an increase in the flow rate often leads to the improvement of efficiency of interphase mass transfer [36,38]. Figure 8B illustrates the efficiency of Z-Tyr-OPNP hydrolysis for reactions catalyzed with the use of MIC monolith performed at 37 °C for 60 min at two flow rates and fixed ratio of molar amounts of catalytic centers to substrate ([Cat]/[S]). As expected, the efficiency of the MIC system was strongly affected by the flow rate: an increase in the flow rate shifted the reaction balance towards product formation by enhancing the number of effective contacts with an increase in the number of recirculation cycles. Catalysis using MIC at a flow rate of 0.5 mL·min^{-1} was less effective than that measured for free chymotrypsin in solution (Figure 8B). However, at a flow rate of 1.5 mL·min^{-1}, the hydrolysis efficacy detected for the MIC monolith was higher than for the native enzyme.

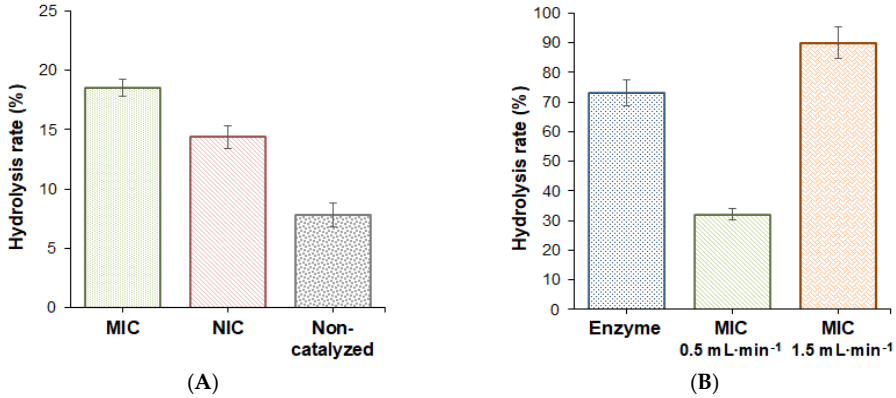

Figure 8. Substrate hydrolysis rate for different systems. Conditions: (**A**) MIC and nonimprinted catalyst (NIC) recirculation mode, flow rate 0.5 mL·min^{-1}, [Cat]/[S] = 1/50; noncatalyzed system: substrate solution under shaking; medium: acetonitrile/0.005 M sodium phosphate buffer (pH 7.8) = 60/40 (% v/v); temperature; 37 °C; time: 240 min; (**B**) recirculation mode for MIC, flow rates 0.5 and 1.5 mL·min^{-1}; the reaction with free enzyme was run under shaking; medium: acetonitrile/0.05 M sodium phosphate buffer (pH 7.8) = 40/60 (% v/v); [Cat]/[S] = 1/20; temperature: 37 °C; time: 60 min.

Considering that heterogeneous catalysis may differ from homogenous one, we prepared a column with immobilized chymotrypsin (IME column) and applied it in flow-through mode to compare the catalysis with mimics under the same conditions. Figure 9 shows the dependences of the Z-Tyr-OPNP hydrolysis rates on time plotted for IME, MIC, and NIC monolithic columns. Both the MIC and NIC monoliths showed the comparable efficiency, which was twice lower than that for IME column.

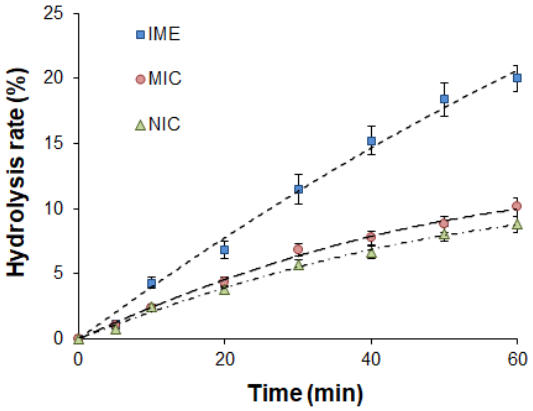

Figure 9. Dependence of hydrolysis rate on time for different catalytic systems. Conditions: recirculation mode, flow rate 0.5 mL·min^{-1}; [Cat]/[S] = 1/80; medium: acetonitrile/0.005 M sodium phosphate buffer (pH 7.8) = 60/40 (% v/v); temperature: 37 °C.

Figure 10 illustrates the dependence of the product amount on time at different catalyst-to-substrate ratios. The enzyme-like behavior was observed for both MIC and NIC systems, that allow us to apply the Michaelis–Menten theory to determine the maximum reaction velocity (V_{max}) and the Michaelis constant (K_M). According to the theory for enzymatically catalyzed processes, a rapid increase in the rate of hydrolysis is observed at the first step of the reaction [37]. After that, the active sites of the enzyme become occupied by substrate molecules, and as a result, the hydrolysis rate reaches a plateau.

In order to determine the kinetic parameters for Z-Tyr-OPNP hydrolysis using MIC and NIC systems, the Michaelis–Menten plots were built. The reaction of Z-Tyr-OPNP hydrolysis was carried out with the use of a 20-100-fold molar excesses of the substrate relative to the catalytic centers in the recirculation mode (Figure S2, the Supplementary Materials). The Michaelis constant (K_M) and the maximum reaction velocity (V_{max}) were determined using a graphical approach based on linearization by Lineweaver–Burk (double reciprocal coordinates, Figure S3, the Supplementary Materials) and Hanes methods ([S]/V on [S] plot). A monolithic column with immobilized chymotrypsin was used as a control. The summarized data on K_M and V_{max} are presented in Table 3. Both mimic systems demonstrated comparable catalytic properties but were inferior in those to natural biocatalyst. The results for the control system were random and poorly reproducible and did not give a Michaelis–Menten plot. An attempt to linearize the data set obtained for the control system gave the positive intercept of x axis. Thus, the Michaelis–Menten theory was not applicable for the disordered polymer system prepared without pre-coordination of functional monomers to mimic the active center of the enzyme.

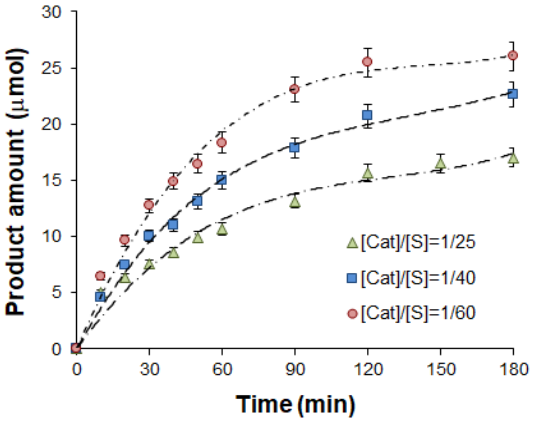

Figure 10. Dependence of product amount on time for the MIC monolith at different substrate concentrations. Conditions: recirculation mode, flow rate 0.5 mL·min^{-1}; medium: acetonitrile/0.005 M sodium phosphate buffer (pH 7.8) = 60/40 (% v/v); temperature: 37 °C.

Table 3. Kinetic parameters for the Z-L-tyrosine p-nitrophenyl ester (Z-Tyr-OPNP) hydrolysis by chymotrypsin mimics and immobilized enzyme (IME). Conditions: reaction medium—acetonitrile/0.005 M sodium phosphate buffer (pH 7.8) = 60/40 (% v/v), 37 °C, 40 min; flow rate was 0.5 mL·min^{-1}. SD values for K_M and V_{max} were from ±5 to ±9%.

Catalytic Column	Flow Rate, mL·min^{-1}	Lineweaver–Burk Method		Hanes Method	
		K_M, mM	V_{max}, µmol·L^{-1}·min^{-1}	K_M, mM	V_{max}, µmol·L^{-1}·min^{-1}
IME	0.5	17	92	26	132
MIC	0.5	37	132	27	106
NIC	0.5	35	139	37	144
MIC	1.5	65	238	46	179

It is known that in contrast to the Lineweaver–Burk method, which suffers from a great magnification of an error in determining the linear reaction velocity at a low substrate concentration, the Hanes method is less prone to this obstacle [39]. The results obtained by Hanes method seem to be more trustworthy. Indeed, in other experiments, IME column demonstrated higher hydrolysis rate than MIC. Obviously, it should have had a higher maximal reaction velocity. In turn, it seems reasonable that MIC, prepared with the use of the template, had K_M close to the enzyme and lower than for the NIC system. Increasing the flow rate to 1.5 mL·min^{-1} favored to the enhancement of catalytic activity (Figure 11) that is in agreement with the experiment performed at fixed [Cat]/[S] ratio (Figure 8B).

To evaluate the ability of mimics to hydrolyze p-nitrophenyl esters of other amino acid derivatives, Fmoc-Ala-OPNP was used as a substrate. The comparison of the hydrolysis efficiency of p-nitrophenyl esters of Tyr- and Ala-derivatives by MIC and NIC monoliths allowed the conclusion that for both mimics, the hydrolysis of the Tyr-based ester was more effective than Ala-based one (Figure 12A). Furthermore, the application of the molecular imprinting technique, involving the use of a hydrophobic template contributed to the formation of a kind of "hydrophobic pocket" (Figure 3), resulted in the more pronounced hydrolysis efficiency by MIC towards Fmoc-Ala-OPNP. However, even for the MIC column, the determined maximum reaction velocity of the hydrolysis reaction of the Ala-based substrate by MIC was twice lower than for Tyr-based one (Figure 12B) that indicates a higher selectivity of MIC to Tyr-based substrates similar to the applied template.

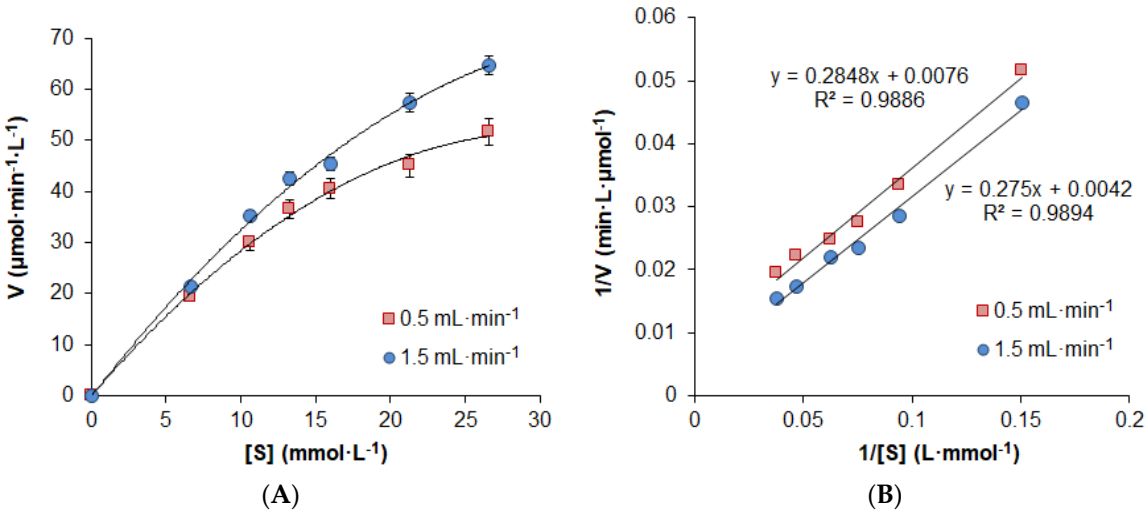

Figure 11. Michaelis–Menten (**A**) and Lineweaver–Burk (**B**) plots for macroporous MIC monolith operated at different flow rates.

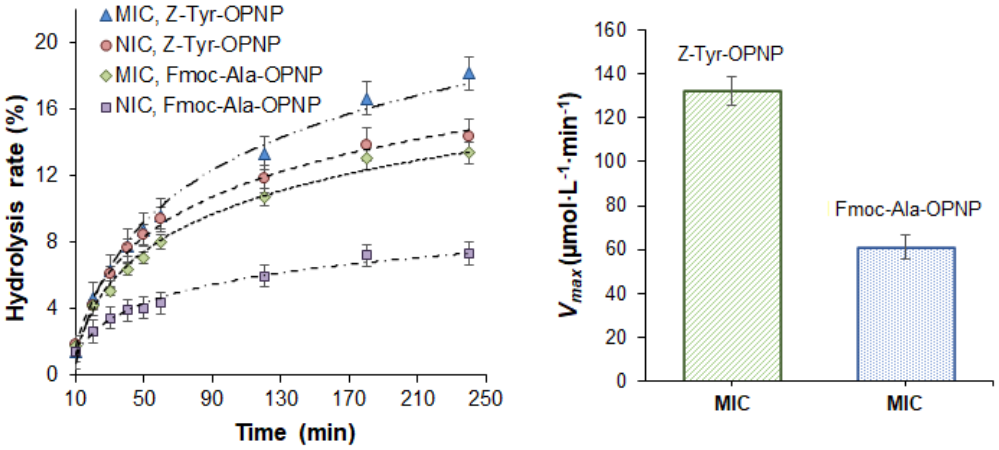

Figure 12. Comparison of the mimic monoliths' activity towards Tyr- and Ala-derivatives: (**A**) dependence of hydrolysis rate on time for MIC and NIC (for reaction conditions, see Figure 8A) and (**B**) maximal reaction velocity for hydrolysis of different substrates by MIC.

It is known that natural biocatalysts are highly effective but only at certain pH and temperature optimum. Deviation from the optimal values can lead to deterioration of the catalytic properties or even their total disappearance due to the distortion of the spatial structure of the enzyme [40]. As seen from Figure 13, an elevation of temperature from 37 to 50 °C increased the catalytic efficiency of the immobilized enzyme during 40 min of the reaction. However, after 60 min, the rate of hydrolysis slowed down and finally decreased from 55% to 45% after 240 min. In turn, as expected, the artificial mimic system demonstrated better stability at elevated temperature. In the case of the MIC monolith, the rate of hydrolysis was doubled with increasing temperature. After 240 min, the hydrolysis rate reached 36% at 50 °C instead of 18% at 37 °C. This result may be related to the enhanced diffusivity of the substrate molecules at elevated temperatures. Contrary to the enzyme active site, the artificial sites are stable and, thus, do not depend on temperature.

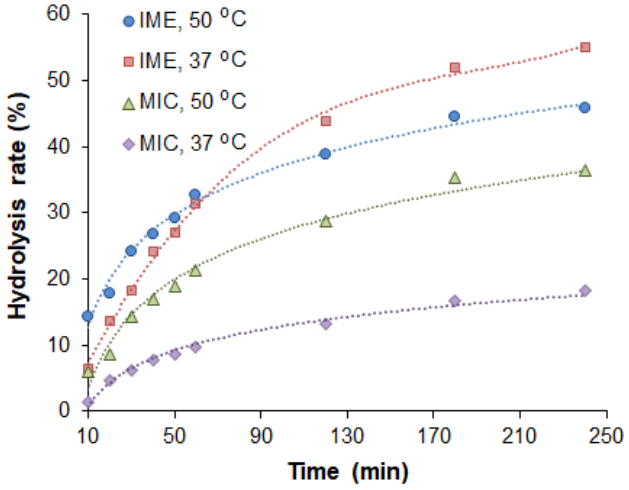

Figure 13. Dependence of hydrolytic efficiency on time at 37 and 50 °C for immobilized enzyme (IME) and MIC monoliths. Conditions: reaction medium—acetonitrile/0.005 M sodium phosphate buffer (pH 7.8) = 60/40 (% v/v); [Cat]/[S] = 1/50; flow rate was 0.5 mL·min^{-1}.

Evaluation of the stability of the MIC column over time showed that the catalytic activity remained constant even after 40 catalytic cycles that indicates high regeneration of the catalyst after use and good stability of artificial catalytic sites.

3. Materials and Methods

3.1. Chemicals and Supplements

The following chemicals were used for preparation of the amino acid derivatives and a template: L-histidine (PanEco, Moscow, Russia), L-serine (Vecton, St. Petersburg, Russia), L-aspartic acid (Vecton, St. Petersburg, Russia), L-tyrosine (BioDuly, Nanjing, China), Fmoc-L-Ala (Sigma-Aldrich, Moscow, Russia), Z-L-tyrosine (Energy Chemical, Zhejiang, China), nicotinic acid (BioDuly, Nanjing, China), methacryloyl chloride (Sigma-Aldrich, Steinheim, Germany), and p-nitrophenol (Interchim, St. Petersburg, Russia), $CoCl_2 \cdot 6H_2O$ (Vecton, St. Petersburg, Russia).

MAA (99%), HEMA (97%), EDMA (98%), PEGDA-700, and DEGDMA (95%) used as monomers as well as 1-dodecanol, toluene, 1,4-butanediol, 1-decanol, cyclohexanol, isooctane, 1-propanol, PEG-600 used as porogens and N,N'-dicyclohexylcarbodiimide (DCC, 99%) were purchased from Sigma-Aldrich (Moscow, Russia). Further, 2,2'-azobisisobutyronitrile (AIBN) used as initiator was a product of Fischer Scientific (Pittsburg, PA, USA). Moreover, 2,4,6-trinitrobenzenesulfonic acid (TNBS, 98%) trihydrate and p-toluenesulfonic acid monohydrate (99%) were purchased from Fluka (Buchs, Switzerland) and BidePharm (Shanghai, China), respectively. All other solvents, salts, and inorganic and small organic compounds used in the work were from ordered from Vecton (St. Petersburg, Russia).

Macroporous monoliths were synthesized inside the stainless-steel housings of 50 mm × 4.6 mm produced by Supelco (Bellefonte, PA, USA). All mobile phases were purified by ultrafiltration through nylon filters with pore size of 0.45 μm produced by Merck Millipore (Moscow, Russia). All sample solutions loaded into the monolithic columns were filtered with the use of MCE or PTFE syringe filters with pore size of 0.22 μm produced by Jet Biofil (Guangzhou, China).

3.2. Methods

3.2.1. Synthesis of Amino Acid-based Monomers (MA-His, MA-Ser, and MA-Asp)

The synthesis of MA-His was carried out according to the protocol published elsewhere [41] with some changes. Briefly, 5.00 g of L-histidine (0.032 mol), 0.20 g of sodium nitrite (0.003 mol), and 30 mL of potassium carbonate solution (water/saturated solution of K_2CO_3 = 95/5 (vol%/vol%)) adjusted to a value of 9.8 (control by a pH meter) with 0.83 g of sodium hydroxide (0.021 mol) were placed into a three-necked flask with a volume of 100 mL. To remove oxygen from the reaction mixture, the synthesis was preceded by passing an inert gas (argon) through the reaction mixture for 10–15 min. Then, the reaction flask was placed in an ice bath (0–2 °C) and 4 mL (0.041 mol) of methacryloyl chloride was added dropwise under stirring of reaction mixture. After that, the reaction was carried out with constant stirring for 2 h at room temperature. At the end of the reaction, the pH of the reaction mixture was adjusted to 7 with 4 M aqueous sodium hydroxide solution. Thereafter, the reaction mixture was extracted to remove unreacted methacryloyl chloride in portions (1/2 of the resulting mixture) with 20 mL of ethyl acetate for each portion. As a result of three repetitions of the extraction, a yellow aqueous solution was obtained, and then, it was evaporated to dryness on a rotary evaporator. Furthermore, 10 mL of methanol was added to the flask to dissolve the product and separate it from salts by filtration. The product dissolved in methanol was precipitated in 750 mL of fry acetone. After two reprecipitations, the isolated yellow hygroscopic solid was placed in a vacuum dryer without heating for 12–14 h. The product yield was 49%. IR (KBr, cm^{-1}): 3409 (–NH stretch.), 1705 (C=O stretch. carboxyl group), 1655 (C=O stretch. amide I), and 1603 (C=C stretch. conjugated with C=O). ^{1}H NMR (D_2O, ppm): 1.8 (3H, singlet, –C=C–CH_3), 2.9–3.1 (2H, multiplet, –C–CH_2–imidazole), 4.4 (1H, triplet, –CH–COOH), 5.3 (1H, singlet, –CH_a=C–), 5.6 (1H, singlet, –CH_b=C–), 7.0 (1H, singlet, ring proton of imidazole at C5), and 8.2 (1H, singlet, imidazole ring proton at C2).

MA-Ser was synthesized and purified in the same manner as MA-His using 0.032 mol of L-serine. The product yield was 50%. IR (KBr, cm^{-1}): 3412 (–NH stretch.), 1709 (C=O val. carboxyl group),

1661 (C=O val. amide I), and 1609 (C=C val. conjugated with C=O). ^{1}H NMR (D_2O, ppm), 1.9 (3H, singlet, –C=C–CH_3), 3.8–3.9 (2H, multiplet, –CH_2–OH), 4.3 (1H, triplet, –CH–COOH), 5.4 (1H, singlet, –CH_a=C–), and 5.7–5.8 (1H, singlet, –CH_b=C–).

MA-Asp was synthesized and purified as described for MA-His using 0.032 mol of L-aspartic acid. In this case, a twofold increase in the amount of sodium hydroxide was required to neutralize the β-carboxyl group of aspartic acid and achieve the required pH value. The product yield was 59%. IR (KBr, cm^{-1}): 3417 (–NH stretch), 1701 (C=O val. carboxyl group), 1659 (C=O val. amide I), and 1603 (C=C val. conjugated with C=O). ^{1}H NMR (D_2O, ppm): 1.8 (3H, singlet, –C=C–CH_3), 2.4–2.7 (2H, multiplet, –C–CH_2–COOH), 4.4 (1H, triplet, –CH–COOH), 5.4 (1H, singlet, –CH_a=C–), and 5.6 (1H, singlet, –CH_b=C–).

3.2.2. Synthesis of Template and Substrates

Template (N-nicotinoyltyrosylbenzyl ester) and substrate (Z-Tyr-OPNP) were synthesized without changes as described elsewhere [19].

The template yield was 35%. IR (KBr, cm^{-1}): 3331 (–NH stretch.), 1737 (C=O stretch. ester), 1663 (C=N stretch. nicotine ring), 1629 (C=O stretch. amide I), and 1514 (C-H def. aromatic ring). ^{1}H NMR ($CDCl_3$, ppm): 3.2 (2H, multiplet, –CH_2–Ph tyrosine); 3.7–3.8 (1H, multiplet, –CH–COOR tyrosine); 5.1 (2H, multiplet –O–CH_2–Ph); 6.7 and 7.0 (2H, multiplet, ring proton of tyrosine); 7.3–7.4 (5H, multiplet, ring proton –O–CH_2–Ph); and 7.5, 8.2, 8.8, and 9.0 (1H, multiplet, annular proton of the nicotine ring).

Z-Tyr-OPNP yield was 72%. IR (KBr, cm^{-1}): 3471 (O–H stretch.), 3315 (–NH stretch.), 1754 (C=O stretch. ester), 1701 (C=O stretch. amide I), and 1522 (C–H def. aromatic ring). ^{1}H NMR (DMSO-d6, ppm): 2.9−3.1 (2H, multiplet, –CH_2–Ph tyrosine), 4.5 (1H, multiplet, –CH–COOR tyrosine), 5.1 (2H, singlet, –O–CH_2–Ph), 6.7 and 7.1 (2H, multiplet, ring proton of tyrosine), 7.3 (5H, multiplet, ring proton of benzyloxycarbonyl), 7.4 and 8.3 (2H, multiplet, ring proton of p-nitrophenol), and 9.3 (1H, singlet, proton of the hydroxyl group of p-nitrophenol).

Fmoc-Ala-OPNP was synthesized using the following procedure. For this, 1.5567 g (0.005 mol) of Fmoc-Ala and 0.6951 g (0.005 mol) of *p*-nitrophenol were placed and dissolved in 25 mL of ethyl acetate freshly distilled over sodium sulfate. The mixture obtained was added to the solution of 1.0599 g (0.005 mol) DCC in 20 mL of freshly distilled ethyl acetate and the reaction medium was left overnight at room temperature under stirring. After that, the formed dicyclohexylurea precipitate was filtered off with a Schott filter and the resulting yellow solution was evaporated on a rotor until a precipitate began to form. Then, the mixture was left at room temperature until the precipitation stopped and the resulting precipitate was separated using a Schott filter. Then, the product on the Schott filter was washed with 50 mL of cold methanol (4–5 °C) and dried in a vacuum for 24 h. The washing and drying procedures were repeated 3 times. Fmoc-Ala-OPNP yield was 51%. FT-IR (cm^{-1}): 3312 (–NH stretch.), 1760 (C=O stretch. ester), 1697 (C=O stretch. amide I), and 1523 (C-H def. aromatic rings). ^{1}H NMR (DMSO-d6, ppm): 1.5 (3H, doublet, –CH–CH_3); 4.3 (1H, triplet, –CH–COOR); 4.4–4.5 (1H and 2H, multiplet, –CH–CH_2–); 7.3 (multiplet), 7.44 (multiplet), 7.7 (multiplet), 7.9 (doublet) (2H, ring protons of the Fmoc benzene rings); 7.4 and 8.3 (2H, doublet, p-nitrophenol ring protons); and 8.1 (1H, doublet, –NH–COOR).

3.2.3. Synthesis of Macroporous Mimic Monoliths

Precisely, 3 mL of a homogeneous polymerization mixture, consisting of functional and cross-linking monomers, cobalt (II) chloride, porogens, and an initiator (AIBN, 1 wt% from total mass of monomers) was purged for 3–5 min with argon and loaded into a housing for in situ polymerization. The filled housing was placed in a water thermostat and polymerized at 70 °C. For details of one-step mimic synthesis and framework synthesis optimization, see Tables S1 and S2, respectively (the Supplementary Materials). After the polymerization, the column with the obtained polymer was connected to a peristaltic pump and washed with a mixture of methanol/hydrochloric

acid = 95/5 (% v/v) until the total removal of cobalt ions (approx. 100 mL) for one-step mimic system. The degree of washing of the material from cobalt ions was monitored spectrophotometrically at 673 nm. The polymer was washed until there was no change in the absorption of the wash solution. After that, the column was washed sequentially with 15 mL of ethanol, 20 mL of ethanol/water = 50/50 (% v/v), and then 20 mL of water. The last procedure was used for washing of monolithic frameworks in the two-step mimic preparation. The flow rate in all cases was 0.5 mL·min^{-1}. All washing solutions were filtered through syringe filters before use.

Before grafting the mimic polymer layer, a weighed portion of cobalt (II) chloride was dissolved in methanol. After that, the weighed portions of monomers, a template, an aliquot of a cross-linking monomer, and a weighed portion of an initiator (AIBN, 1 wt% from the total mass of monomers) were sequentially introduced into cobalt chloride solution. Homogenization of the mixture after the addition of each component was carried out using an ultrasonic bath. The resulting polymerization mixture was filtered through a Schott filter and purged with argon for 3–5 min to remove oxygen. The prepared mixture was left for 30 min and after that injected with a syringe into macroporous monolithic framework, in situ prepared in the stainless-steal column. The grafting was carried out at 70 °C during different time (Table 1). The resulting columns were washed using a peristaltic pump in the same way as described above. The control monolith was prepared in a similar manner but without the addition of cobalt (II) chloride.

3.2.4. Characterization of Macroporous Monoliths

The pore characteristics (average pore size and porosity) of all macroporous monoliths were determined based on the data of hydrodynamic permeability calculated according to the Poiseuille–Darcy law as described elsewhere [42].

The surface morphology of the obtained macroporous monoliths was investigated using scanning electron microscopy (SEM) with secondary electron detection. Images were recorded at a magnification 1000× and 5000× using a scanning electron microscope Zeiss AURIGA Laser (Oberkochen, Germany).

The mechanical stability of macroporous monoliths to the mobile phase flow was investigated by the installation of columns into a Shimadzu LC-20 Prominence HPLC system (Kyoto, Japan) and measuring the backpressure at different flow rates of the mobile phase (acetonitrile/water=60/40, % v/v). The flow rate was varied from 0.5 to 10 mL·min^{-1}.

The quantity of double bonds was determined by Raman spectroscopy with the use of a Nicolet 6700 Fourier spectrometer (Thermo Scientific, Waltham, MA, USA) with an NXR Raman attachment at room temperature. Experimental parameters—spectral resolution 4 cm^{-1}, number of scans—800, exciting laser—Nd: YVO4, 1064 nm, and laser power—1 W. The spectra were taken from the rounded surfaces of the cylinders of monoliths placed on the bases. Dimensions of cylinders were height—3–5 mm and diameter—2–3 mm. The relative quantity (%) of double bonds was calculated by referring the areas of the characteristic bands for each sample, corresponding to the vibrations of the C=C-groups, to the areas of the characteristic bands of the CH-groups for the corresponding samples.

The quantitative determination of catalytic centers was carried after hydrolysis of grafted functional polymer. For this, 0.1 g, of grafted monolith, prewashed with ethyl alcohol and dried, was ground, placed in a 25 mL round-bottom flask, and refluxed for 24 h with 10 mL of 0.1 M aqueous hydrochloric acid under constant stirring. Then, the solution was cooled to room temperature, the pH was adjusted to 6–7 using an aqueous solution of sodium hydroxide (0.4 M) and evaporated to dryness on a rotary evaporator. Furthermore, 5 mL of water was added to the obtained dry residue and stirred for 1 h at room temperature. The resulting aqueous solution of amino acid(s) was filtered from the polymer particles with a glass fiber syringe filter. The qualitative analysis of amino acid(s) was carried out with use of 2,4,6-trinitrobenzenesulfonic acid (TNBS) specific to primary amino groups. Analysis was performed as follows. Precisely, 1.5 mL of 0.0125 M borate buffer solution (pH = 9.4) and 0.1 mL of 8% aqueous TNBS solution were added to 0.5 mL of the analyzed solution, and kept for 50 min at room temperature. After that, 1.5 mL of 0.01 M citrate buffer solution (pH = 4.8) was added and

mixed, and the optical density of the solution was determined at λ = 425 nm against the control sample (prepared in the same way, but with the use of 0.5 mL of water instead of the analyzed solution). To determine the amount of amino acid(s) in the solution, the corresponding calibration curves were preliminarily built (Figure S4, the Supplementary Materials).

3.2.5. Chymotrypsin Immobilization

25 mg (10^{-6} mol) of the α-chymotrypsin was dissolved in 1.5 mL of 0.0125 M borate buffer solution, pH = 8.5. The resulted solution was loaded into macroporous monolithic column based on poly(glycidylmethacrylate-co-ethylene glycol dimethacrylate). The monolithic column had the following characteristics: length 50 mm, diameter 4.6 mm, average pore size 1590 nm, and void volume 0.67 mL. The immobilization was carried out under shaking at 37 °C for 16 h. After that, the columns with the immobilized enzyme were washed by the same buffer solution, an aqueous solution of hydrochloric acid (pH 2), and again with buffer solution to remove unreacted enzyme. The volume of each washing portion was 3 mL. The amount of bound enzyme was determined by the Lowry-Folin assay. The amount of immobilized enzyme was calculated as difference between quantity of enzyme in initial solution and enzyme quantity determined in solutions after immobilization and washing. The amount of immobilized enzyme was equal to 3.4 mg per column. The average pore size after chymotrypsin immobilization practically did not change.

3.2.6. Evaluation of Catalytic Properties

After preparation of monolithic column, the test materials were washed using a peristaltic pump with 10 mL of acetonitrile/water = 50/50 (% v/v), and then, the liquid was removed from the column and blown with air for 2 min.

A catalytic reaction was carried out by pumping a substrate solution through the column in a recirculation mode using a peristaltic pump. The molar ratios of substrate/catalytic centers ranged from 20 to 100. The volume of reaction medium was equal to 5.6 mL for NIC and IME and 10 mL for NIC. The reaction mixtures for the catalytic reaction represented the substrate solution in acetonitrile/0.005 M sodium phosphate buffer (pH 7.8) = 60/40 (% v/v). The reaction was performed at 37 °C at different flow rates depending on experiment (0.5 or 1.5 mL·min^{-1}). Time of catalytic reaction ranged from 10 to 240 min. The amount of the resulting reaction product (p-nitrophenol) was determined using the previously plotted calibration curve (Figure S5, the Supplementary Materials). The absorbance of p-nitrophenol in solution was measured at a wavelength of 405 nm. The determination of Michaelis constant (K_M) and maximum reaction velocity (V_{max}) was performed with use of the initial velocity of the catalytic reaction calculated at 40 min. Lineweaver–Burk and Hanes coordinates were used for linearization.

4. Conclusions

Flow-through macroporous polymer monoliths containing catalytic centers mimicking chymotrypsin active sites were obtained by surface grafting of Co(II)-coordinated assembly of N-methacryloyl-L-serine, N-methacryloyl-L-histidine, and N-methacryloyl-L-aspartic acid as monomers, with or without template. Both kinds of mimics prepared in the presence or absence of the template demonstrated the catalytic enzyme-like properties towards Z-Tyr-OPNP that followed Michaelis–Menten kinetics. Polymerization of the same monomers in the absence of Co-ions provided a disordered polymer layer, which demonstrated poor catalytic properties different from the Michaelis–Menten kinetics. The efficiency of the developed macroporous mimic monoliths depended on the flow rate of recirculation of the substrate solution that is typical for immobilized enzyme reactors based on monoliths. The hydrolysis efficiency for the mimic system operating at a flow rate of 1.5 mL·min^{-1} was higher than that for soluble enzyme under the same conditions but lower than for the immobilized chymotrypsin operating in flow-through mode. At the same time, an elevation of the temperature to 50 °C led to a decrease in the hydrolysis efficiency for the immobilized enzyme, while it

increased for the mimic system. The mimics obtained were characterized by excellent stability of artificial catalytic sites. The catalytic activity kept constant even after 40 catalytic cycles of hydrolysis. Despite the fact that mimics were less efficient than immobilized enzymes in catalysis at standard conditions for the enzyme, they can surpass natural biocatalysts in long-term stability and applicability to harsher reaction conditions.

Supplementary Materials: The following are available online at http://www.mdpi.com/2073-4344/10/12/1395/s1, Table S1: Compositions of polymerization mixtures tested for the one-step synthesis of macroporous polymer monolith containing catalytic centers mimicking chymotrypsin active site. Table S2: Compositions of polymerization mixtures tested for the synthesis of macroporous monolithic framework. Figure S1: Raman spectra of macroporous polyEDMA synthesized during different polymerization time. Figure S2: Scheme of catalysis performance in the recirculation mode. Figure S3: Lineweaver–Burk plots for hydrolysis of Z-L-tyrosine p-nitrophenyl ester (Z-Tyr-OPNP) by macroporous nonimprinted mimic (NIC) (A) and immobilized enzyme (IME) (B) monoliths, and hydrolysis of Fmoc-Ala-OPNP by macroporous imprinted mimic (MIC) monolith (C). Figure S4: Calibration plot for L-His and mixture of amino acids (L-Ala, L-His, and L-Ser) determination with the use of 2,4,6-trinitrobenzenesulfonic acid (TNBS) solution. Figure S5: Calibration plot for p-nitrophenol.

Author Contributions: Conceptualization—E.K.-V. and T.T.; investigation—M.S., O.S., and D.T.; methodology—M.S.; formal analysis—M.S., D.T., and O.S., data curation—M.S. and E.K.-V.; visualization—E.K.-V.; scientific supervision—E.K.-V.; writing—original draft preparation, E.K.-V.; writing—review and editing, M.S., T.T., and E.K.-V. All authors have read and agreed to the published version of the manuscript.

Funding: This research received no external funding.

Acknowledgments: The Center for Chemical Analysis and Materials Research, Center for Geo-Environmental Research and Modeling (GEOMODEL), and Interdisciplinary Center for Nanotechnology of the Research Park of SPbU are acknowledged for IR- and Raman spectroscopy and SEM, respectively.

Conflicts of Interest: The authors declare no conflict of interest.

References

1. Singh, R.; Kumar, M.; Mittal, A.; Mehta, P.K. Microbial enzymes: Industrial progress in 21st century. *3 Biotech* **2016**, *6*, 1–15. [CrossRef]
2. Chapman, J.; Ismail, A.E.; Dinu, C.Z. Industrial Applications of Enzymes: Recent Advances, Techniques, and Outlooks. *Catalysts* **2018**, *8*, 238. [CrossRef]
3. Alexander, C.; Davidson, L.; Hayes, W. Imprinted polymers: Artificial molecular recognition materials with applications in synthesis and catalysis. *Tetrahedron* **2003**, *59*, 2025–2057. [CrossRef]
4. Mathew, D.; Thomas, B.; Devaky, K.S. Design, synthesis and characterization of enzyme-analogue-built polymer catalysts as artificial hydrolases. *Artif. Cells Nanomed. Biotechnol.* **2019**, *47*, 1149–1172. [CrossRef]
5. Huang, Y.; Liu, C.; Pu, F.; Liu, Z.; Ren, J.; Qu, X. A GO–Se nanocomposite as an antioxidant nanozyme for cytoprotection. *Chem. Commun.* **2017**, *53*, 3082–3085. [CrossRef] [PubMed]
6. Li, S.; Liu, X.; Chai, H.; Huang, Y. Recent advances in the construction and analytical applications of metal-organic frameworks-based nanozymes. *TrAC Trends Anal. Chem.* **2018**, *105*, 391–403. [CrossRef]
7. Shi, C.; Li, Y.; Gu, N. Iron-Based Nanozymes in Disease Diagnosis and Treatment. *ChemBioChem* **2020**, *21*, 2722–2732. [CrossRef] [PubMed]
8. Mathew, D.; Thomas, B.; Devaky, K.S. Geometrical effect of 3D-memory cavity on the imprinting efficiency of transition-state analogue-built artificial hydrolases. *Polym. Bull.* **2017**, *75*, 3883–3896. [CrossRef]
9. Zeng, L.; Cui, H.; Chao, J.; Huang, K.; Wang, X.; Zhou, Y.; Jing, T. Colorimetric determination of tetrabromobisphenol A based on enzyme-mimicking activity and molecular recognition of metal-organic framework-based molecularly imprinted polymers. *Microchim. Acta* **2020**, *187*, 142. [CrossRef] [PubMed]
10. Zhang, N.; Xu, Y.; Li, Z.; Yan, C.; Mei, K.; Ding, M.; Ding, S.; Guan, P.; Qian, L.; Du, C.; et al. Molecularly Imprinted Materials for Selective Biological Recognition. *Macromol. Rapid Commun.* **2019**, *40*, e1900096. [CrossRef]
11. Cheng, Z.; Zhang, L.; Li, Y. Synthesis of an Enzyme-like Imprinted Polymer with the Substrate as the Template, and Its Catalytic Properties under Aqueous Conditions. *Chem. Eur. J.* **2004**, *10*, 3555–3561. [CrossRef]
12. Chen, Z.; Hua, Z.; Wang, J.; Guan, Y.; Zhao, M.; Li, Y. Molecularly imprinted soluble nanogels as a peroxidase-like catalyst in the oxidation reaction of homovanillic acid under aqueous conditions. *Appl. Catal. A Gen.* **2007**, *328*, 252–258. [CrossRef]

13. Li, J.; Zhu, M.; Wang, M.; Qi, W.; Su, R.; He, Z. Molecularly imprinted peptide-based enzyme mimics with enhanced activity and specificity. *Soft Matter* **2020**, *16*, 7033–7039. [CrossRef] [PubMed]
14. Philip, C.; Devaky, K. Multiwalled carbon nanotubes with surface grafted transition state analogue imprints as chymotrypsin mimics for the hydrolysis of amino acid esters: Synthesis and kinetic studies. *Mol. Catal.* **2017**, *436*, 276–284. [CrossRef]
15. Díaz-Díaz, G.; Antuña-Jiménez, D.; Blanco-López, M.C.; Lobo-Castañón, M.J.; Miranda-Ordieres, A.J.; Tuñón-Blanco, P. New materials for analytical biomimetic assays based on affinity and catalytic receptors prepared by molecular imprinting. *TrAC Trends Anal. Chem.* **2012**, *33*, 68–80. [CrossRef]
16. Czulak, J.; Jakubiak-Marcinkowska, A.; Trochimczuk, A. Polymer Catalysts Imprinted with Metal Ions as Biomimics of Metalloenzymes. *Adv. Mater. Sci. Eng.* **2013**, *2013*, 1–9. [CrossRef]
17. Wang, R.; Pan, J.; Qin, M.; Guo, T. Molecularly imprinted nanocapsule mimicking phosphotriesterase for the catalytic hydrolysis of organophosphorus pesticides. *Eur. Polym. J.* **2019**, *110*, 1–8. [CrossRef]
18. Tadi, K.K.; Motghare, R.V.; Ganesh, V. Electrochemical detection of epinephrine using a biomimic made up of hemin modified molecularly imprinted microspheres. *RSC Adv.* **2015**, *5*, 99115–99124. [CrossRef]
19. Lele, B.; Kulkarni, M.; Mashelkar, R. Molecularly imprinted polymer mimics of chymotrypsin. *React. Funct. Polym.* **1999**, *39*, 37–52. [CrossRef]
20. Arrua, R.D.; Strumia, M.C.; Igarzabal, C.I.A. Macroporous Monolithic Polymers: Preparation and Applications. *Materials* **2009**, *2*, 2429–2466. [CrossRef]
21. Svec, F. Porous polymer monoliths: Amazingly wide variety of techniques enabling their preparation. *J. Chromatogr. A* **2010**, *1217*, 902–924. [CrossRef] [PubMed]
22. Patrushev, Y.; Yudina, Y.; Sidelnikov, V. Monolithic rod columns for HPLC based on divinylbenzene-styrene copolymer with 1-vinylimidazole and 4-vinylpyridine. *J. Liq. Chromatogr. Relat. Technol.* **2018**, *41*, 458–466. [CrossRef]
23. Andjelković, U.; Tufegdžić, S.; Popović, M. Use of monolithic supports for high-throughput protein and peptide separation in proteomics. *Electrophoresis* **2017**, *38*, 2851–2869. [CrossRef] [PubMed]
24. Rathnasekara, R.; Khadka, S.; Jonnada, M.; El Rassi, Z. Polar and nonpolar organic polymer-based monolithic columns for capillary electrochromatography and high-performance liquid chromatography. *Electrophoresis* **2016**, *38*, 60–79. [CrossRef]
25. Kurganov, A.A. Monolithic column in gas chromatography. *Anal. Chim. Acta* **2013**, *775*, 25–40. [CrossRef]
26. Wang, R.; Li, W.; Chen, Z. Solid phase microextraction with poly(deep eutectic solvent) monolithic column online coupled to HPLC for determination of non-steroidal anti-inflammatory drugs. *Anal. Chim. Acta* **2018**, *1018*, 111–118. [CrossRef]
27. Krenkova, J.; Lacher, N.A.; Svec, F. Highly Efficient Enzyme Reactors Containing Trypsin and Endoproteinase LysC Immobilized on Porous Polymer Monolith Coupled to MS Suitable for Analysis of Antibodies. *Anal. Chem.* **2009**, *81*, 2004–2012. [CrossRef]
28. Liu, X.; Ouyang, C.; Zhao, R.; Shangguan, D.; Chen, Y.; Liu, G. Monolithic molecularly imprinted polymer for sulfamethoxazole and molecular recognition properties in aqueous mobile phase. *Anal. Chim. Acta* **2006**, *571*, 235–241. [CrossRef]
29. Zhu, J.; Chen, D.; Ai, Y.; Dang, X.; Huang, J. A dummy molecularly imprinted monolith for selective solid-phase microextraction of vanillin and methyl vanillin prior to their determination by HPLC. *Microchim. Acta* **2017**, *184*, 1161–1167. [CrossRef]
30. Antipchik, M.; Dzhuzha, A.; Sirotov, V.; Tennikova, T.; Korzhikova-Vlakh, E. Molecularly imprinted macroporous polymer monolithic layers for L-phenylalanine recognition in complex biological fluids. *J. Appl. Polym. Sci.* **2020**. [CrossRef]
31. *Monolithic Materials: Preparation, Properties and Applications*; Elsevier BV: Amsterdam, The Netherlands, 2003.
32. Blow, D.M. Structure and mechanism of chymotrypsin. *Acc. Chem. Res.* **1976**, *9*, 145–152. [CrossRef]
33. Gráf, L.A.; Szilágyi, L.A.; Venekei, I.A. Chymotrypsin. In *Handbook of Proteolytic Enzym*; Elsevier Ltd.: Oxford, UK, 2013; pp. 2626–2633.
34. Vlakh, E.G.; Korzhikov, A.V.; Hubina, A.V.; Tennikova, T.B. Molecular imprinting: A tool of modern chemistry for the preparation of highly selective monolithic sorbents. *Russ. Chem. Rev.* **2015**, *84*, 952–980. [CrossRef]
35. Xie, S.; Svec, F. Design of reactive porous polymer supports for high throughput bioreactors: Poly(2-vinyl-4,4-dimethylazlactone-co-acrylamide-co-ethylene dimethacrylate) monoliths. *Biotechnol. Bioeng.* **1999**, *62*, 30–35. [CrossRef]

36. Ponomareva, E.A.; Volokitina, M.V.; Vinokhodov, D.O.; Korzhikova-Vlakh, E.; Tennikova, T. Biocatalytic reactors based on ribonuclease A immobilized on macroporous monolithic supports. *Anal. Bioanal. Chem.* **2012**, *405*, 2195–2206. [CrossRef] [PubMed]
37. Berg, J.M.; Tymoczko, J.L.; Stryer, L. *Biochemistry*, 6th ed.; W.H. Freeman: New York, NY, USA, 2006; pp. 241–260.
38. Volokitina, M.V.; Vlakh, E.G.; Platonova, G.A.; Vinokhodov, D.O.; Tennikova, T. Polymer monoliths as efficient solid phases for enzymatic polynucleotide degradation followed by fast HPLC analysis. *J. Sep. Sci.* **2013**, *36*, 2793–2805. [CrossRef]
39. Enzyme Biocatalysis: Principles and Applications. *Focus Catal.* **2009**, *2009*, 8. [CrossRef]
40. Bayramoglu, G.; Salih, B.; Arica, M.Y. Catalytic Activity of Immobilized Chymotrypsin on Hybrid Silica-Magnetic Biocompatible Particles and Its Application in Peptide Synthesis. *Appl. Biochem. Biotechnol.* **2019**, *190*, 1224–1241. [CrossRef]
41. Yilmaz, V.; Yilmaz, H.; Arslan, Z.; Leszczynski, J. Novel Imprinted Polymer for the Preconcentration of Cadmium with Determination by Inductively Coupled Plasma Mass Spectrometry. *Anal. Lett.* **2016**, *50*, 482–499. [CrossRef]
42. Vlakh, E.G.; Maksimova, E.F.; Tennikova, T.B. Monolithic polymeric sorbents for high-performance chromatography of synthetic polymers. *Polym. Sci. Ser. B* **2013**, *55*, 55–62. [CrossRef]